

Street Layout Design via Conditional Adversarial Learning

Lehao Yang, Long Li, Qihao Chen, Jiling Zhang, Tian Feng, Wei Zhang
Zhejiang University
Hangzhou, Zhejiang, China

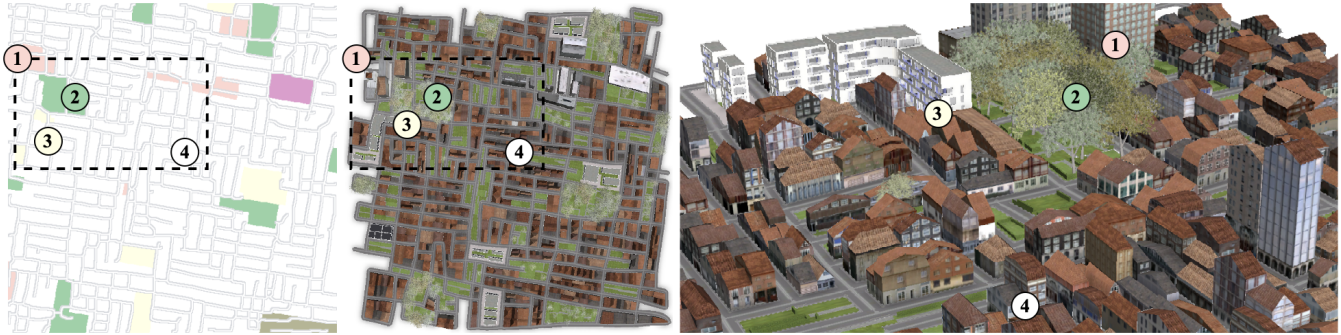


Figure 1: An urban street layout designed by our method (left), and its corresponding three-dimensional virtual environment (middle: top view; right: isometric view). Land use types are identified (1: commercial; 2: parkland; 3: education; 4: residential).

ABSTRACT

Designing high-quality urban street layouts has long been in high demand, but entangles notable challenges. Conventional methods based on deep generative models are yet to fill the gap on integrating both natural and socioeconomic factors in the design loop. In this paper, we propose a novel urban street layout design method based on conditional adversarial learning. Specifically, a conditional generative adversarial network trained on a real-world dataset synthesizes street layout images from the feature map, into which an autoencoder fuses a set of natural and socioeconomic data for a region of interest; The following extraction module generates high-quality street layout graphs corresponding to the synthesized images. Experiments and evaluations suggest that the proposed method outputs various urban street layouts that are visually and structurally alike their real-world counterparts, which can be used to support the creation of high-quality urban virtual environments.

CCS CONCEPTS

• **Computing methodologies** → **Computer graphics; Modeling and simulation; Computer vision.**

KEYWORDS

street layout design, urban modeling, image synthesis, graph generation

ACM Reference Format:

Lehao Yang, Long Li, Qihao Chen, Jiling Zhang, Tian Feng, Wei Zhang. 2023. Street Layout Design via Conditional Adversarial Learning. In *Proceedings of Make sure to enter the correct conference title from your rights confirmation emai (Conference acronym 'XX)*. ACM, New York, NY, USA, 9 pages. <https://doi.org/XXXXXXX.XXXXXXX>

1 INTRODUCTION

Cities are where massive people live and socialize in the real world. An ineffective urban street network limits a city's capability to support smooth travel and transport, enabling street layout design to become a critical task in the area of urban planning. Meanwhile, the gaming industry has also regarded street layout design as an emerging topic in recent years, for visually and structurally sound street networks contribute to immersive and engaging user experience in the virtual urban environments. Being essential to the above-mentioned fields, this challenging task requires professionals to contemplate various factors towards high-quality street layouts given the complexity of cities [28].

The process of street layout design is often time-consuming and tedious, requiring significant knowledge and expertise. Intensive attempts have somewhat allowed users to focus on high-level goals in street layout design. For example, the rule-based methods [5, 23, 30] adopt procedural models for quick generation; the example-based methods [2, 21, 32] rely on structurally decomposing and statistically analysing real-world data; and the optimisation-based [11, 24, 31] encapsulate the task in an optimization process being subject to different costs. These traditional methods accomplish the task driven by natural and socioeconomic factors closely related to city development, but are yet to significantly disengage user intervention (e.g., rules, parameters, and goals) from the process.

The revolutionary development of deep learning techniques has enabled automatic generation of customized high-quality street layouts under less user intervention. Specifically, deep generative models extract structural and textural features from a large amount of data on real-world street networks, and fuse these features for street layout design. For example, generative adversarial network (GAN) [12] and its variants [15, 20] can be trained to map a random noise to street layouts replicating the style of the original patch [27], or synthesize street layouts being aware of user-given

conditions (e.g., sketches, junction guidance, and topographic information) [8–10]; and graph generative models with neural networks iteratively predict the next node connected to an existing node conditioned on the graph representing the current street layout, where street segments and intersections are respectively regarded as edges and nodes [7]. Although these methods have demonstrated promising performances, obvious limitations can be observed about their adaptability to both natural and socioeconomic factors. In urban planning, the local terrain influences the expanding of streets considerably, and the distribution of population and the pattern of land use dominates travel demands that the street network aims to serve [28]. The dependence of street layout design on natural and socioeconomic conditions has been incompletely considered in the current methods based on deep generative models, which is worth exploring.

To fill the above-mentioned gap, we propose a novel method for urban street layout design based on conditional adversarial learning, which is driven by both natural and socioeconomic data. In particular, our method first adopts an autoencoder [4] to encode the input rasterized data on elevation, population density and land use into a feature map; a conditional GAN (cGAN) [15, 20] trained on the real-world dataset then takes as input the feature map and synthesizes street layout images in regard to the corresponding natural and socioeconomic conditions; and the following extraction module constructs and optimizes a street layout graph from each rasterized street layout for vectorization. Experiments and evaluations suggest that the proposed method can design street layouts resembling the street patterns in the corresponding urban regions with various details and demonstrating similar characteristics in terms of connectivity, street density, and traffic accessibility compared to their real-world counterparts. Meanwhile, the output street layouts are able to reflect the input conditions on elevation, population density and land use. Furthermore, we employ ArcGIS CityEngine¹ to create three-dimensional urban virtual environments from example outputs, which illustrates the effectiveness of our method.

The contributions of this work can be summarized as, (1) an end-to-end deep generative model for street layout image synthesis from fused natural and socioeconomic data; (2) an effective street layout extraction module for street layout graph generation from a synthesized street layout image; and (3) experiments and evaluations showing the proposed method's capability of designing various street layouts in regard to the input conditions while being similar to the real-world scenarios.

2 RELATED WORK

Traditional Methods. Rule-based methods have been widely used to solve the street layout design problem, given their strength in quick generation, especially since the pioneer work [23] introduced *L-systems* [25], a forward procedural modeling technique originally for plant modeling, to urban modeling and had later developed into ArcGIS CityEngine for commercial use. Chen et al. [6] applied tensor fields to the procedural modeling of street layouts. Vanegas et al. [30] presented an inverse procedural modeling system for generating plausible street layouts satisfying certain

design indicators. Beneš et al. [5] proposed a procedural modeling technique for growing local urban streets driven by simulating trade-based traffic with neighboring cities. Although rule-based methods enable compact and efficient street layout design with pre-defined grammars and insignificant storage, they usually require professional knowledge and expertise in relevant fields (e.g., urban planning, geography, and transport engineering). The parameters of grammars also need careful configuration by users for desirable outputs, which is uneasy to novices.

Some of earlier studies focus on *example-based* methods for street layout design. Aliaga et al. [2] proposed an urban layout synthesis algorithm based on the information provided by street intersections and aerial imagery. Nishida et al. [21] presented an interactive tool allowing the generation of street layouts with details and styles extracted from existing ones. Example-based methods ask for less user requirement compared to the rule-based regarding professional knowledge and expertise, but their outputs are excessively similar, sometimes even identical, to the source data, demonstrating the drawback on variety of design.

In the recent decade, *optimization-based* methods have gradually become a preferable solution to street layout design. Yang et al. [31] integrated a global optimization module in their hierarchical splitting algorithm to ensure the fairness and regularity of the generated streets. Peng et al. [24] proposed to create street layouts from high-level functional specifications with integer programming driven by topological constraints and scores. Feng et al. [11] devised a crowd-aware layout design method based on stochastic optimization against crowd flow costs. Optimization-based methods can generate street layouts in an effective and uncomplicated way, but only if objective functions are appropriately formulated to represent user-given design goals and constraints. Otherwise, seeking optimal street layouts can be significantly difficult.

Deep Generative Models. Recent methods based on deep generative models solve the problem following diverse strategies. *Graph-based* methods characterize a street layout as a planar graph comprising nodes and edges, and thus formulate the problem as graph generation. Chu et al. [7] proposed Neural Turtle Graphics (NTG), based on an encoder-decoder architecture where the encoder recurrent neural network (RNN) encodes incoming paths into a node and the decoder RNN creates outgoing nodes and connecting edges. Despite the success in learning local street patterns, NTG can hardly process large-scale street layouts. Owaki et al. [22] improved the encoder and decoder neural networks in NTG to predict the attributes of both streets and blocks. These methods concentrate on the topology of a street layout as graph, whereas the proposed method aims to design street layouts adapted to natural and socioeconomic conditions.

The other *image-based* methods formulate street layout design as image synthesis. Hartmann et al. [27] firstly proposed StreetGAN, a GAN-based method synthesizing textures to represent street layouts from a noise image, which has a limited generative capability and is prone to model collapse [3, 18]. Fang et al. [10] devised an image complement method predicting street layouts having a limited size in a user-specified region. More recently, Kelvin et al. [16] introduced a cGAN-based tool for generating street map tiles from a user-defined sketch, which however lacks details on the output

¹<https://www.esri.com/en-us/arcgis/products/arcgis-cityengine/overview>

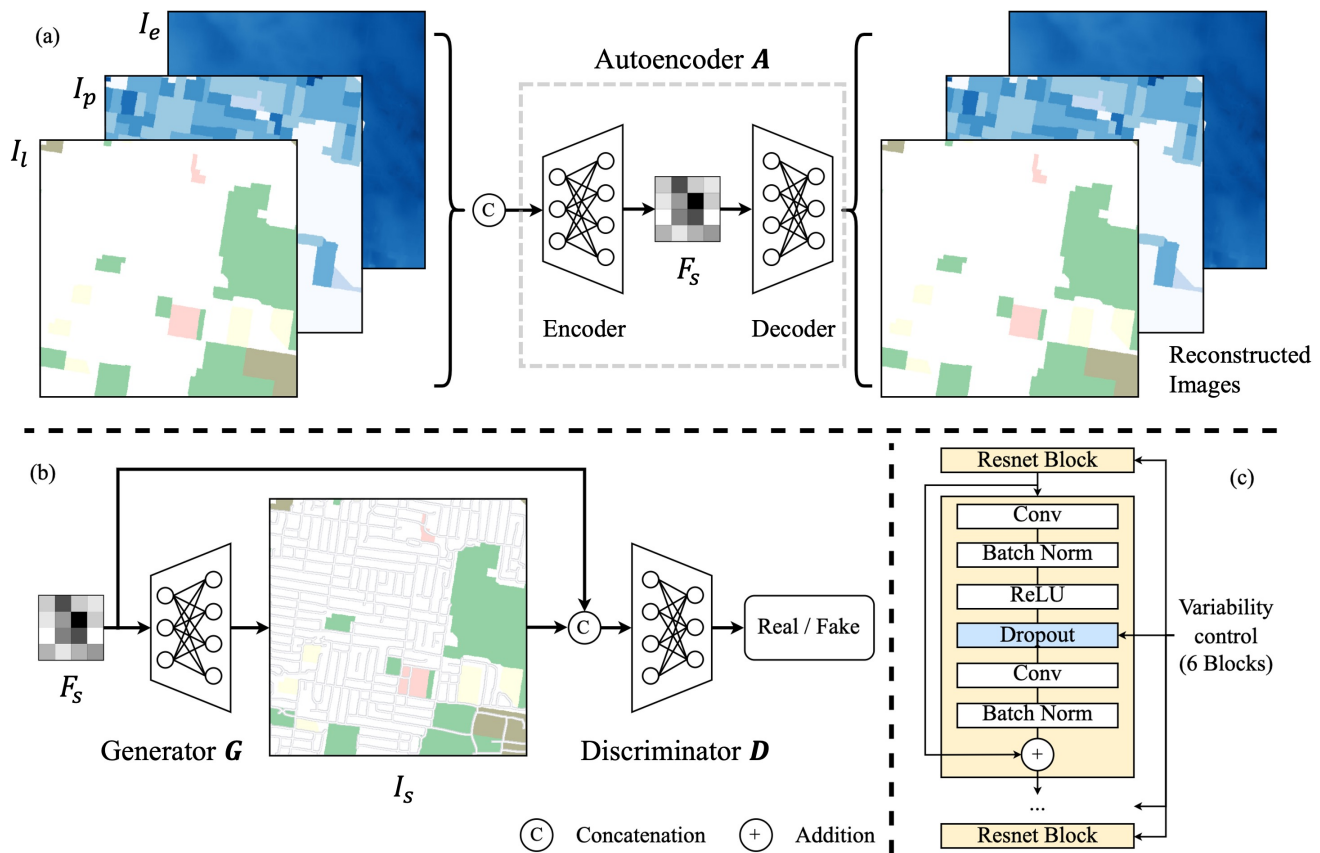


Figure 2: Architecture of the street layout image synthesis module. (a) The autoencoder \mathcal{A} encodes the input images I_e , I_p , and I_l into a feature map F_s . (b) The generator \mathcal{G} maps F_s to a street layout image I_s , and the discriminator \mathcal{D} distinguishes the images corresponding the real-world street layouts from the synthesized. (c) The structure of \mathcal{G} comprises includes dropout layers for controlling the variability of the synthesized images.

quality. Fang et al. [8, 9] devised cGAN-based methods for street layout design given planning guidance defined by users and contextual information closely related to topography. Although our method is similarly cGAN-based, it employs data fusion to simultaneously integrate the conditions on elevation, population density, and land use in the design loop, which echos the rule in urban planning that street layout design requires the contemplation of natural and socioeconomic factors.

3 OVERVIEW

The proposed method comprises a *synthesis* module and an *extraction* module. The synthesis module adopts an autoencoder to produce a feature map F_s by fusing three single-band images I_e , I_p , and I_l that project the information on elevation, population density, and land use, respectively, of a region of interest \mathcal{R} . Subsequently, a cGAN trained on a real-world dataset takes as input F_s and synthesizes a single-band image I_s , which represents a street layout in raster data (see Section 4).

The extraction module initially processes the synthesized image I_s into an enhanced image \hat{I}_s that filters the unwanted artifacts.

Afterwards, a planar graph G_s is constructed from \hat{I}_s by comparing each pixel and its neighbors, followed by optimizing it into the final output graph \hat{G}_s , which represents a street layout in vector data (see Section 5).

Once \hat{G}_s meets the user's expectation, it can be easily converted into a standard geospatial data format (e.g., SHAPEFILE²) and thus serves three-dimensional urban virtual scene creation using a mainstream urban modeling platform (e.g., ArcGIS CityEngine). Otherwise, our method can regenerate street layouts with updated details but still corresponding to the same input data for user choice.

4 STREET LAYOUT IMAGE SYNTHESIS

The synthesis module aims to synthesize street layouts from natural and socioeconomic conditions, where all these data are represented as images. Therefore, our synthesis task can be formulated as predicting an output y from an input x .

Inspired by a two-player zero-sum minimax game, GAN [12] is a deep generative models comprising a generator \mathcal{G} and a discriminator \mathcal{D} . Focusing on the mapping from a random noise z to a *fake*

²<https://doc.arcgis.com/en/arcgis-online/reference/shapefiles.htm>

image \hat{y} (i.e., $\hat{y} = \mathcal{G}(z)$), \mathcal{D} is trained to differentiate a *real* image y from \hat{y} , whereas \mathcal{G} aims to synthesize \hat{y} indistinguishable to \mathcal{D} . To incorporate other input information, cGAN [20] enables a slightly different process: its \mathcal{G} synthesizes \hat{y} from a user-given condition x in addition to z (i.e., $\hat{y} = \mathcal{G}(x, z)$). In this way, the input-output relationship can be explored to support controlled generation.

Our street layout synthesis module \mathcal{S} is cGAN-based, as following the recent practices on terrain synthesis [15], street map tiles generation [16], and topography-aware street network modeling [9]. Unlike the original cGAN, our \mathcal{S} takes as input only a condition set $x = \{I_e, I_p, I_l\}$, but without any random noise z . This design follows our observation that random noise usually leads to the degeneration of the output quality, because the model may simply learn how to remove the noise rather than extract the underlying relationship serving our task, which is consistent with the findings of previous studies [15, 19]. In the dataset for training \mathcal{S} , each condition set $x = \{I_e, I_p, I_l\}$ corresponds to an image y representing a real-world street network, which enables a one-to-one mapping. The limited number of samples available for each condition set, however, result in that \mathcal{S} may struggle to learn both stable structural features and textural differences from real images.

As an image contains limited variation but considerable redundant information and even noise, we employ an autoencoder \mathcal{A} to process the input images I_e, I_p , and I_l projecting the information on elevation, population density, and land use, given its outstanding capability of compressing and downscaling data [4, 14]. Specifically, \mathcal{A} is composed of an encoder, which compresses I_e, I_p , and I_l into a feature map F_s , and a decoder, which reconstructs the images from the feature map. This process of data compression can be formulated as,

$$F_s = \mathcal{A}(I_e, I_p, I_l). \quad (1)$$

Conventional GANs usually construct the discriminator \mathcal{D} as a classifier trained with the Sigmoid cross-entropy loss, which sometimes causes vanishing gradients and leads to instability and unsatisfactory quality in synthesized images [3]. To address this issue, we adopt a least-squares loss [18] to train the generator \mathcal{G} , whose objective function is formulated as,

$$\min \mathcal{L}_{\mathcal{G}} = \mathbb{E}_{F_s} [(\mathcal{D}(\mathcal{G}(F_s), F_s) - 1)^2], \quad (2)$$

and the objective function of \mathcal{D} is formulated as,

$$\min \mathcal{L}_{\mathcal{D}} = \frac{1}{2} \mathbb{E}_{x, F_s} [(\mathcal{D}(x, F_s) - 1)^2] + \frac{1}{2} \mathbb{E}_{F_s} [(\mathcal{D}(\mathcal{G}(F_s), F_s))^2]. \quad (3)$$

Figure 2 shows the architecture of our street layout image synthesis module, which comprises an autoencoder \mathcal{A} , a generator \mathcal{G} , and a discriminator \mathcal{D} . We adopt convolution-BatchNorm-ReLu [26] network blocks and residual blocks [13] with a dropout layer [29], as illustrated in Figure 2 (c).

4.1 Autoencoder

Our autoencoder \mathcal{A} compress the concatenated input images I_e, I_p , and I_l of size $512 \times 512 \times 3$ into a feature map F_s of size 64×64 , which captures salient image features. Specifically, the encoder includes an input layer, downsampling blocks, residual blocks, and an output layer, where the downsampling blocks progressively reduce the dimensionality and size of the input and the residual blocks enhance the network's ability to extract useful features; and the decoder

is structurally symmetrical to the encoder, comprising an input layer, residual blocks, upsampling blocks, and an output layer. The encoder's output layer produces F_s . Our autoencoder \mathcal{A} enables efficient compression of the input images while preserving their critical information for street layout image synthesis.

4.2 Generator

Our generator \mathcal{G} takes as input the feature maps F_s without any random noise, and includes an input layer, downsampling blocks, residual blocks, upsampling blocks, and an output layer. As dropout layers can be used to prevent overfitting and improve the network's generalization [29], we introduce dropout layers to six residual blocks and two upsampling blocks, which enables \mathcal{G} to structurally or texturally control the synthesized image I_s . In particular, a street layout's structure and connectivity can be controlled by randomly masking a portion of high-level semantic features in the residual blocks and of low-level semantic features in the upsampling blocks, respectively. By avoiding the use of random noise and introducing dropout layers, our method can synthesize high-quality street layout images with various structures and connectivities.

4.3 Discriminator

Reasonable streets should be geometrically continuous lines or curves, which are represented as high-frequency features in a street layout image. Conventional GAN discriminators evaluate the average quality of images at a global level, which may cause image blurring, or even training failure. In contrast, our discriminator \mathcal{D} follows the design of PatchGAN [15] that focuses on patch-scale structures for fine-grained evaluation of image quality, which ensures the quality of synthesized street layout images.

5 STREET LAYOUT GRAPH EXTRACTION

The output of the street layout image synthesis module is a grayscale image I_s by the generator \mathcal{G} from the feature map F_s , which needs converting to a planar graph for downstream tasks, such as statistical analysis, urban modeling, and data visualization. Our street layout graph extraction module includes three steps: image processing, graph construction, and graph optimization.

5.1 Image Processing

We first convert the street layout image I_s to a binary image using a threshold value of 127, where streets are represented by pixels in white with value of 255 and other pixels in black with value of 0 correspond to non-street areas. The following morphological expansion operation aims to remove artifacts, including tiny holes, disconnected segments, and parallel streets, and produces a cleaned binary image for street layout skeleton extraction [33]. Iterative operations of morphological expansion and skeleton extraction can enhance the quality of the street layout skeleton in the processed image \hat{I}_s without compromising the structural integrity. Please note that the colors adopted in Figure 3 are for visualization only, where streets are in black and non-street areas in white.

5.2 Graph Construction

From the processed image \hat{I}_s representing a street layout skeleton (see Figure 3 (a)), we construct a planar graph $G_s = \{V, E\}$ with a

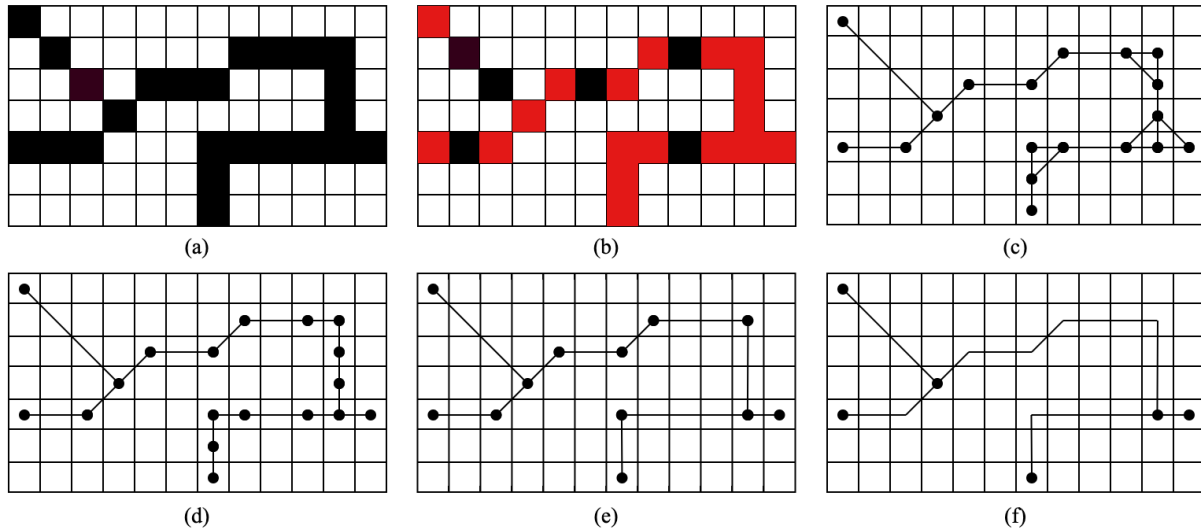


Figure 3: Process of the street layout graph extraction. (a) The initial street layout skeleton, where streets are represented in black and non-street areas in white. (b) The street layout skeleton after vertex selection, where invalid vertices are in red. (c) The constructed street layout graph G_s , where isosceles right triangles exist at street corners. (d) The street layout graph after the removal of isosceles right triangles. (e) The street layout graph after the removal of redundant vertices. (f) The optimized street layout graph \hat{G}_s .

vertex set $V = \{v_i\}$ and an edge set $E = \{e_{ij}\}$. Each vertex v_i encodes a spatial location $[x_i, y_i]^T$, and each edge $e_{ij} = \overline{v_i v_j}$ denotes a street segment. We define a pixel with value of 255 as valid, and check the 8 neighboring pixels for each valid pixel. Each valid pixel p_i will be regarded as a vertex v_i added to V if its neighboring pixels meets one of the following criteria:

- the existence of 1 valid pixel;
- the existence of more than 2 valid pixels; and
- the existence of 2 valid pixels, to which p_i cannot be connected in a straight line.

We traverse \hat{I}_s to find all valid vertices that satisfying any of the above criteria (see Figure 3 (b)). For each vertex v_i , we locate its adjacent vertices v_j and add an edge $e_{ij} = \overline{v_i v_j}$ to E , which produces an initial street layout graph G_s .

5.3 Graph Optimization

The constructed street layout graph G_s may exhibit undesirable isosceles right triangles at street corners, as shown in Figure 3 (c). We find each of such triangles by traversing the vertices and then remove its longest edge (see Figure 3 (d)). Besides, the intermediate graph usually contains a substantial number of redundant vertices hardly contributing to the street layout. For simplification, we eliminate such vertices (see Figure 3 (d)) and merge corresponding edges to obtain the final street layout graph \hat{G}_s , as shown in Figure 3 (f).

6 EXPERIMENTS

We implemented the proposed method using Python and PyTorch on a workstation with a NVIDIA RTX A5000 graphics card (24 GB memory), and created three-dimensional urban virtual environments for showcase using ArcGIS CityEngine on a laptop with

a NVIDIA GeForce RTX 3080Ti graphics card (12 GB memory). Evaluations were all conducted on the street layout graphs. For visualization, we assigned colors to the street layouts according to the land use types.

6.1 Implementation Details

To train the synthesis module \mathcal{S} , we pre-trained the autoencoder \mathcal{A} by optimizing the L_2 loss between the original input images and the reconstructed ones using the Adam solver [17] with momentum parameters $\beta_1 = 0.5$ and $\beta_2 = 0.999$. The learning rate was set to 0.0002 and decayed to one-tenth for every 300 steps. We selected the best autoencoder by performance on an independent test set. Then, we used the encoder while freezing all of its parameters to train the cGAN. During the training of the cGAN, we alternated between one gradient descent step on the discriminator \mathcal{D} and one step on the generator \mathcal{G} . The dropout rate in \mathcal{D} was 0.5, where \mathcal{D} performed binary classification for each 64×64 patch of the input images.

During the testing, we adopted the encoder of \mathcal{A} and \mathcal{G} to synthesize street layout images. Unlike traditional methods, we incorporated dropout layers in testing to enhance the image quality using the dropout rate ranging from 0.5 to 0.99. We found that the dropout rate of 0.95 corresponded to street layout images with stable structural integrity and textural variability.

6.2 Dataset Preparation

We produced a real-world street layout dataset based on the map data from OpenStreetMap (OSM)³. Specifically, each street in

³<https://www.openstreetmap.org>

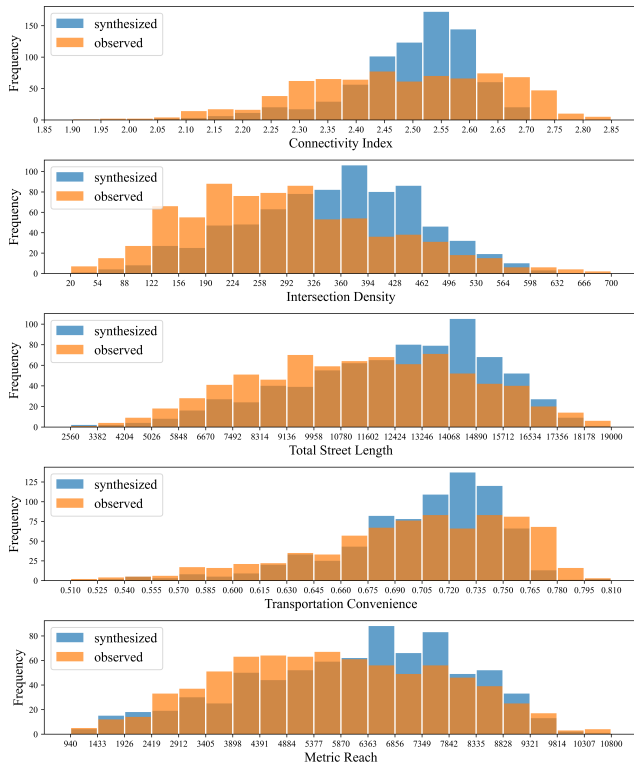


Figure 4: Comparison between the street layouts output from the proposed method (blue) and the real-world ones (orange) in statistical evaluation.

the OSM map data is tagged with a specific *highway* type representing its category. We only selected streets tagged *highway*-categories: *motorway*, *primary*, *secondary*, *tertiary*, *residential*, *living street*, or *pedestrian*, from three major Australian cities (i.e., Sydney, Melbourne, and Brisbane). Due to incomplete data tagging in those underpopulated regions, we only adopted the map data for the populated regions to ensure adequate representation.

The map data (i.e., vectorized street layouts) in SHAPEFILE was rasterized using the OSGEO library⁴, involving the projection of the street layouts into the Web Mercator coordinate system in meters. All street layouts images were cropped to 512×512 patches with a 5m spatial resolution and street width of 3 pixels. In particular, streets were represented by pixels in white with value of 255, and non-street areas by pixels in black with value of 0. In addition, we rasterized the 2021 Census data⁵ into 512×512 images that projected the information on elevation, population density and land use corresponding to the collected street layouts. Our dataset consists of 2586 pairs of street layout images and natural / socioeconomic images, of which 70% were for training and 30% for testing.

⁴<https://gdal.org/api/python/osgeo.html>

⁵<https://www.abs.gov.au/census>

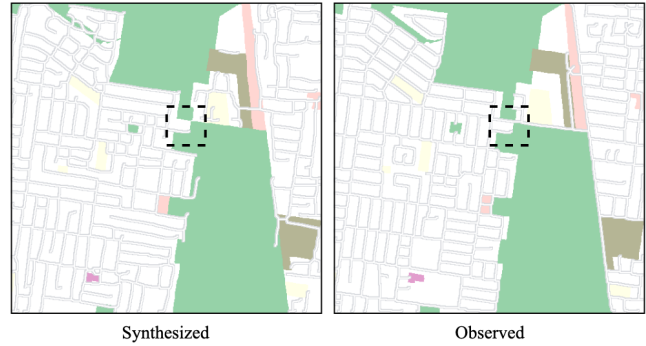


Figure 5: Comparison between an example street layout output from the proposed method (left) and its corresponding real-world counterpart (right).

6.3 Statistical Evaluation

In the field of urban planning, numerous studies have focused on street layout qualitative evaluation regarding the capability to support various urban functions (e.g. pedestrian and vehicular movements). As an urban street layout can be represented as a planar graph, the topological and geometric attributes may resemble its quality and pattern. For example, the central area of a city with a radial layout is supposed to exhibit high connectivity and provide easy access, whereas residential communities are generally located around dead-end streets or T-junctions to reduce traffic for privacy and security.

Therefore, we adopted the following the statistical metrics [1] to assess the topological and geometric attributes of a street layout regarding connectivity and pattern encoding.

Connectivity Index (t_{ci}). We defined the connectivity index as the average vertex degree of the corresponding graph to measure the quality of a street layout in connecting destinations, which is formulated as,

$$t_{ci}(G) = \frac{\sum_i degree(v_i)}{number(v_i)}. \quad (4)$$

In particular, we focused on vertices with degrees other than 2. It is noteworthy that urban planning guidelines usually employ a minimum connectivity index of 1.4 [28], which underscores the importance of ensuring adequate connectivity in a street layout to support efficient transportation and facilitate access to key destinations.

Intersection Density (t_{id}). The metric of intersection density serves as a quantitative measure of the number of intersections present within a given patch layout, defined as the total number of vertices with degrees greater than 2. This metric provides valuable insights into the connectivity and accessibility of a street layout and can inform decision-makers of either optimizing the efficiency and functionality of transportation infrastructure.

Total Street Length (g_{sl}). The effectiveness of transportation infrastructure is intrinsically linked to the total length of streets. Areas with high population density, for instance, often exhibit densely distributed streets, while rural areas are typically characterized by a sparse network.

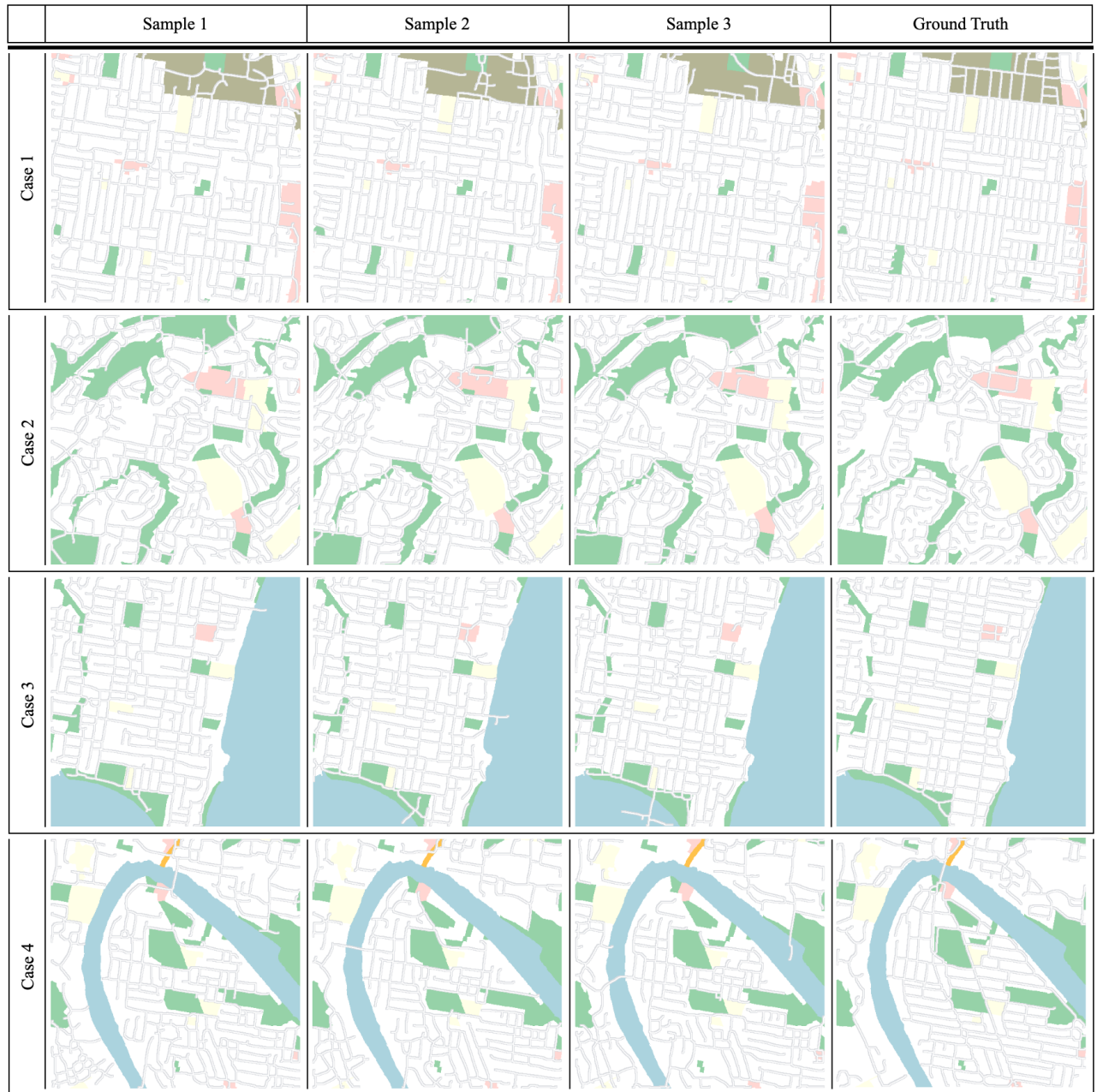


Figure 6: Visualization of the street layouts outputs output from the proposed method and the real-world ones in 4 cases. Land use types are identified (brown: industrial; green: parkland; red: commercial; yellow: education; white: residential; orange: transport; blue: water).

Transportation Convenience (g_{tc}). Transportation convenience measures the easiness of traveling from source s to destination d . Suppose $d_E(s, d)$ refers to the Euclidean distance between $s \rightarrow d$ and $d_D(s, d)$ to the shortest graph distance, the transportation convenience between s and d is formulated as,

$$g_{tc}(s, d) = \frac{d_E(s, d)}{d_D(s, d)}. \quad (5)$$

For a street layout, we randomly sampled 100 sets of source and destination locations and calculated the average transportation convenience. To avoid local estimation, source and destination locations were required to have a minimal Euclidean distance ($d_E(s, d) > 0.25km$ in our implementation).

Metric Reach (g_{mr}). As a well-established concept in urban planning literature, metric reach is defined as the total length of streets

that can be accessed by traveling a given distance (0.5km in our implementation) in all possible directions, without retracing any paths, which provides a comprehensive assessment of the accessibility and connectivity of a street layout.

Figure 4 compares statistical evaluation results between the synthesized street layouts by our method and the real-world street layouts. In all metrics, the synthesized street layouts demonstrate that the distribution of the synthesized street layout is consistent with the real-world ones. Specifically, our model prefers to synthesize streets with high connectivity and numerous intersections, which can be derived from the connectivity index and intersection density, where larger connectivity index represents more streets connected to an intersection. This indicates that the synthesized street layout is able to support a heavy travel demand and maintain efficient transportation. From total street length and metric reach it can be concluded that the synthesized street layout has denser streets and better accessibility compared to the real-world. The synthesized street layouts do not outperform the real-world ones in terms of high transportation convenience. Further analysis reveals that some of the synthesized street layouts lack a bridge-like structure, as shown in Figure 5. Specifically, the synthesized street layout is divided into two separate pieces on the left and right. Consequently, we observe a reduction in both connectivity index and transportation convenience. In summary, our model demonstrates its ability to learn the geometric and topological properties of the real-world street layout.

6.4 Visual Evaluation

We also evaluated the generative capability of our method from a visual perspective. In each of the four cases, we synthesized 1000 street layouts and selected three of them for presentation (see Figure 6). We controlled the variability of the synthesized street layouts by setting the dropout rate. In particular, we adopted the dropout rate of 0.95 in the 6 network blocks, which could maintain the image quality and ensure the variability (see Figure 7).

Case 1. As a grid-like street layout, it is characterized by containing rectangular patterns of varying sizes, like a chessboard. It can be noticed that the synthesized street layout is similar in structure but has a varied texture compared to its real-world counterpart. In particular, residential areas have more rectangular streets than those of other land use types.

Case 2. As a curved street layout, it contains a lot of curved streets and dead ends. It can be noted that the synthesized street layout reproduces the curved streets of high quality. In addition, it captures the different land use types accurately. The large parkland area indicates a strong correlation between the synthesized street layout and the input population density. Specifically, the streets are significantly sparse on a parkland area, as there are almost no residents.

Case 3. As a street layout surrounded by water, no streets are placed over the water, whereas the synthesized street layout has a grid-like pattern alike its real-world counterpart.

Case 4. As a street layout including river, it can be observed that the synthesized street layout is divided into two parts with

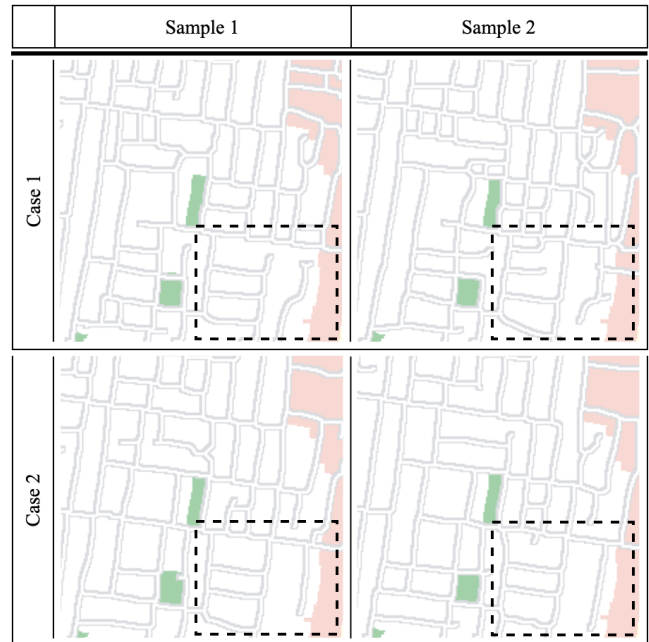


Figure 7: Visualization of variability control by the proposed method. Land use types are identified (brown: industrial; green: parkland; red: commercial; yellow: education; white: residential. The black dotted box is the interest area).

bridges generated to maintain connectivity. In addition, the streets are deliberately bypass parkland areas and the river.

In addition, we changed the position, number and parameters of the dropout layer in the network blocks to control the variability of the synthesized street layouts, as shown in Figure 7. For Case 1, we added 6 dropout layers to high-level features, randomly hiding 95% of the feature information, which led to a structural change in the street layout. For Case 2, we added 1 dropout layer to the low-level features, randomly hiding 95% of the feature information, which led to a slight change in the texture of the street layout.

The street layouts output from our method can reflect the conditions on elevation, population density and land use. We used ArcGIS CityEngine to create three-dimensional urban virtual environments from the synthesized street layouts, illustrating the effectiveness of our method (see Figure 1).

7 CONCLUSION

In this paper, we proposed an end-to-end deep generative model for street layout image synthesis from fused natural and socioeconomic data, and an effective street layout extraction module generating corresponding graphs. Experiments and evaluations suggested that our method could generate various street layouts representing the input conditions, while being similar to the real-world cases. Furthermore, we utilized the output street layouts for three-dimensional urban virtual environment creation, which showed the method's promise in urban modeling. In future work, we are to explore the design of street layouts with increased properties (e.g., levels and modes).

REFERENCES

- [1] Sawsan AlHalawani, Yong-Liang Yang, Peter Wonka, and Niloy J. Mitra. 2014. What Makes London Work Like London? *Computer Graphics Forum* 33, 5 (Aug. 2014), 157–165. <https://doi.org/10.1111/cgfg.12441>
- [2] Daniel G. Aliaga, Carlos A. Vanegas, and Bedrich Benes. 2008. Interactive Example-Based Urban Layout Synthesis. In *ACM SIGGRAPH Asia 2008 Papers* (Singapore) (*SIGGRAPH Asia '08*). Association for Computing Machinery, New York, NY, USA, Article 160, 10 pages. <https://doi.org/10.1145/1457515.1409113>
- [3] Martin Arjovsky, Soumith Chintala, and Léon Bottou. 2017. Wasserstein GAN. <https://doi.org/10.48550/ARXIV.1701.07875>
- [4] Pierre Baldi. 2011. Autoencoders, Unsupervised Learning and Deep Architectures. In *Proceedings of the 2011 International Conference on Unsupervised and Transfer Learning Workshop - Volume 27* (Washington, USA) (*UTLW'11*). JMLR.org, 37–50.
- [5] Jan Beneš, Alexander Wilkie, and Jaroslav Krivánek. 2014. Procedural Modelling of Urban Road Networks. *Computer Graphics Forum* 33, 6 (2014), 132–142. <https://doi.org/10.1111/cgfg.12283>
- [6] Guoning Chen, Gregory Esch, Peter Wonka, Pascal Müller, and Eugene Zhang. 2008. Interactive Procedural Street Modeling. *ACM Trans. Graph.* 27, 3 (aug 2008), 1–10. <https://doi.org/10.1145/1360612.1360702>
- [7] Hang Chu, Daiqing Li, David Acuna, Amlan Kar, Maria Shugrina, Xinkai Wei, Ming-Yu Liu, Antonio Torralba, and Sanja Fidler. 2019. Neural Turtle Graphics for Modeling City Road Layouts. In *2019 IEEE/CVF International Conference on Computer Vision (ICCV)*. 4521–4529. <https://doi.org/10.1109/ICCV.2019.00462>
- [8] Zhou Fang, Ying Jin, and Tianren Yang. 2022. Incorporating Planning Intelligence into Deep Learning: A Planning Support Tool for Street Network Design. *Journal of Urban Technology* 29, 2 (2022), 99–114. <https://doi.org/10.1080/10630732.2021.2001713>
- [9] Zhou Fang, Jiaxin Qi, Lubin Fan, Jianqiang Huang, Ying Jin, and Tianren Yang. 2022. A topography-aware approach to the automatic generation of urban road networks. *International Journal of Geographical Information Science* 36, 10 (2022), 2035–2059. <https://doi.org/10.1080/13658816.2022.2072849>
- [10] Zhou Fang, Tianren Yang, and Ying Jin. 2020. DeepStreet: A deep learning powered urban street network generation module. <https://doi.org/10.48550/ARXIV.2010.04365>
- [11] Tian Feng, Lap-Fai Yu, Sai-Kit Yeung, KangKang Yin, and Kun Zhou. 2016. Crowd-Driven Mid-Scale Layout Design. *ACM Trans. Graph.* 35, 4, Article 132 (jul 2016), 14 pages. <https://doi.org/10.1145/2897824.2925894>
- [12] Ian Goodfellow, Jean Pouget-Abadie, Mehdi Mirza, Bing Xu, David Warde-Farley, Sherjil Ozair, Aaron Courville, and Yoshua Bengio. 2020. Generative Adversarial Networks. *Commun. ACM* 63, 11 (oct 2020), 139–144. <https://doi.org/10.1145/3422622>
- [13] Kaiming He, Xiangyu Zhang, Shaoqing Ren, and Jian Sun. 2015. Deep Residual Learning for Image Recognition. <https://doi.org/10.48550/ARXIV.1512.03385>
- [14] G. E. Hinton and R. R. Salakhutdinov. 2006. Reducing the Dimensionality of Data with Neural Networks. *Science* 313, 5786 (July 2006), 504–507. <https://doi.org/10.1126/science.1127647>
- [15] Phillip Isola, Jun-Yan Zhu, Tinghui Zhou, and Alexei A. Efros. 2017. Image-To-Image Translation With Conditional Adversarial Networks. In *Proceedings of the IEEE Conference on Computer Vision and Pattern Recognition (CVPR)*.
- [16] Lin Ziwen Kelvin and Anand Bhojan. 2020. Procedural Generation of Roads with Conditional Generative Adversarial Networks. In *ACM SIGGRAPH 2020 Posters* (Virtual Event, USA) (*SIGGRAPH '20*). Association for Computing Machinery, New York, NY, USA, Article 12, 2 pages. <https://doi.org/10.1145/3388770.3407422>
- [17] Diederik P. Kingma and Jimmy Ba. 2014. Adam: A Method for Stochastic Optimization. <https://doi.org/10.48550/ARXIV.1412.6980>
- [18] Xudong Mao, Qing Li, Haoran Xie, Raymond Y. K. Lau, Zhen Wang, and Stephen Paul Smolley. 2016. Least Squares Generative Adversarial Networks. <https://doi.org/10.48550/ARXIV.1611.04076>
- [19] Michael Mathieu, Camille Couprie, and Yann LeCun. 2015. Deep multi-scale video prediction beyond mean square error. <https://doi.org/10.48550/ARXIV.1511.05440>
- [20] Mehdi Mirza and Simon Osindero. 2014. Conditional Generative Adversarial Nets. [arXiv:1411.1784 \[cs.LG\]](https://arxiv.org/abs/1411.1784)
- [21] G. Nishida, I. Garcia-Dorado, and D. G. Aliaga. 2016. Example-Driven Procedural Urban Roads. *Comput. Graph. Forum* 35, 6 (sep 2016), 5–17. <https://doi.org/10.1111/cgfg.12728>
- [22] Takashi Owaki and Takashi Machida. 2022. Road Network Generation with City Block Attributes Using Link Attribute Aggregation. In *2022 IEEE 25th International Conference on Intelligent Transportation Systems (ITSC)*. IEEE. <https://doi.org/10.1109/itsc55140.2022.9921784>
- [23] Yoav I. H. Parish and Pascal Müller. 2001. Procedural Modeling of Cities. In *Proceedings of the 28th Annual Conference on Computer Graphics and Interactive Techniques (SIGGRAPH '01)*. Association for Computing Machinery, New York, NY, USA, 301–308. <https://doi.org/10.1145/383259.383292>
- [24] Chi-Han Peng, Yong-Liang Yang, Fan Bao, Daniel Fink, Dong-Ming Yan, Peter Wonka, and Niloy J. Mitra. 2016. Computational Network Design from Functional Specifications. *ACM Trans. Graph.* 35, 4, Article 131 (jul 2016), 12 pages. <https://doi.org/10.1145/2897824.2925935>
- [25] P Prusinkiewicz. 1986. Graphical Applications of L-Systems. In *Proceedings on Graphics Interface '86/Vision Interface '86* (Vancouver, British Columbia, Canada). Canadian Information Processing Society, CAN, 247–253.
- [26] Alec Radford, Luke Metz, and Soumith Chintala. 2015. Unsupervised Representation Learning with Deep Convolutional Generative Adversarial Networks. <https://doi.org/10.48550/ARXIV.1511.06434>
- [27] Klein Reinhard, Wessel Raoul, Weinmann Michael, and Hartmann Stefan. 2017. StreetGAN: Towards Road Network Synthesis with Generative Adversarial Networks, In International Conference on Computer Graphics, Visualization and Computer Vision. *International Conference on Computer Graphics*.
- [28] Yossi Sheffi. 1984. *Urban Transportation Networks: Equilibrium Analysis with Mathematical Programming Methods*. Prentice-Hall.
- [29] Nitish Srivastava, Geoffrey Hinton, Alex Krizhevsky, Ilya Sutskever, and Ruslan Salakhutdinov. 2014. Dropout: a simple way to prevent neural networks from overfitting. *The journal of machine learning research* 15, 1 (2014), 1929–1958.
- [30] Carlos A. Vanegas, Ignacio Garcia-Dorado, Daniel G. Aliaga, Bedrich Benes, and Paul Waddell. 2012. Inverse Design of Urban Procedural Models. *ACM Trans. Graph.* 31, 6, Article 168 (nov 2012), 11 pages. <https://doi.org/10.1145/2366145.2366187>
- [31] Yong-Liang Yang, Jun Wang, Etienne Vouga, and Peter Wonka. 2013. Urban Pattern: Layout Design by Hierarchical Domain Splitting. *ACM Trans. Graph.* 32, 6, Article 181 (nov 2013), 12 pages. <https://doi.org/10.1145/2508363.2508405>
- [32] Qizhi Yu and Anthony Steed. 2012. Example-based Road Network Synthesis. In *EG 2011 - Short Papers*. Eurographics Association, Cagliari, Italy.
- [33] T. Y. Zhang and C. Y. Suen. 1984. A fast parallel algorithm for thinning digital patterns. *Commun. ACM* 27, 3 (March 1984), 236–239. <https://doi.org/10.1145/357994.358023>

Received 20 February 2007; revised 12 March 2009; accepted 5 June 2009